Biointerface Research in Applied Chemistry
Platinum Open Access Journal (ISSN: 2069-5837)

Article
Volume 12, Issue 4, 2022, 4307 - 4316
https://doi.org/10.33263/BRIAC124.43074316

Calcium Pretreated *Pinus Roxburghii* Wood Biochar for Adsorptive Removal of Fluoride from Aqueous Solution

Tarun Kumar Yadav [1], Abhishek , Bablu Prasad [3], Deepak Singh [4], Kumar Suranjit Prasad [1,*]

[1] Centre of Environmental Studies, Institute of Inter-Disciplinary Studies, University of Allahabad, Prayagraj, Uttar, Pradesh, 211002; tarunyadav1512@gmail.com (T.K.Y.);
[2] Department of Geology, Faculty of Science, The Maharaja Sayajirao University of Baroda, Vadodara, 390002; hi2abhishekkumar@gmail.com (A.K.);
[3] Department of Environmental Studies, Faculty of Science, The Maharaja Sayajirao University of Baroda, Vadodara- India; akashganga812@gmail.com (B.P.);
[4] Department of Environmental Science, Deshbandhu College, University of Delhi, New Delhi 110019; deepaksingh1947@gmail.com (D.S.);
* Correspondence: ksuranjit@allduniv.ac.in (K.S.P.);

Scopus Author ID 56507879300

Received: 26.06.2021; Revised: 30.07.2021; Accepted: 2.08.2021; Published: 15.08.2021

Abstract: Fluorosis due to consuming an elevated amount of fluoride-containing groundwater is believed to be a serious public health-related issue. A calcium pretreated wood of *Pinus roxburghii* was converted into biochar and examined for fluoride uptake from an aqueous solution. Further characterization of biochar was performed using FT-IR and SEM EDAX analysis. Results suggested the involvement of different functional groups of biochar in the sorption process. Scanning microscopy and elemental analysis showed the porous structure of biochar with an appreciably high loading of fluoride ions. Sorption of fluoride occurred due to chemical interaction between functional groups that existed over the surface of biochar. Sorption was found to be spontaneous and exothermic. The prepared adsorbent holds good promises to be used as an agent for defluoridation.

Keywords: fluoride; adsorption; biochar; *Pinus roxburghii*; FT-IR.

1. Introduction

Water is one of the essential natural resources on earth for sustaining life and the environment, which we have thought to be available in profusion and everlasting [1]. When present in high or sometimes even in low amounts, certain ions are a serious issue as their presence makes the groundwater inappropriate for drinking as well as other purposes [2]. Fluoride is a strongly electronegative ion, commonly found in combination with calcium or sodium, forming naturally occurring compounds in soil and water [3]. Fluoride beyond the threshold concentrations (0.6 to 1.5mgL^{-1}) has been a major setback in several parts of the world [4]. Considerable increase in fluoride concentrations in surface and groundwater has been reported from several regions of India and its neighboring country, Bangladesh, over the past few years [5]. Fluoride is believed to be the chief pollutant of groundwater worldwide. Including India, about 25 countries worldwide are suffering from high fluoride content in the groundwater [6]. Similar or larger problems are anticipated in other countries, including China, Ethiopia, and Uzbekistan [7]. Fluoride levels in regions of Ethiopia are as high as 33 mg L^{-1} [8], and levels of up to 2800 mgL^{-1} have been measured in soda lakes in Kenya [9] and Tanzania [10].

Fluorine is the most electronegative and most reactive. Owing to its high reactivity, fluorine is not found in nature in its elemental state and exists as fluorides [11,12] Fluoride-bearing rocks such as fluorite, fluorapatite, fluorspar, cryolite, and hydroxylapatite are the major source of fluoride in groundwater [13].

Various methods have been reported for the removal of fluoride from water; consequently, different sorbent materials such as natural, synthetic, and biomass have been investigated to remove fluoride from aqueous solutions [14]. Lately, a number of new adsorbents have been investigated for fluoride adsorption[15]. For example, La(II) and Y(III)-impregnated alumina, aluminum-impregnated carbon and lanthanum-impregnated silica-gel [16], Fe(III)-Al (III) hydroxide floc [17], Kaolinite [18], La-Ce modified alumina [19], Si modified with rice husk [20], raw rice husk [21] have been utilized for fluoride adsorption. Chai *et al*. (2013) developed a novel adsorbent of sulfate-doped Fe_3O_4/Al_2O_3 nanoparticles with magnetic separability to remove fluoride from drinking water. A novel magnetic nanosized adsorbent using hydrous aluminum oxide embedded with Fe_3O_4 nanoparticle ($Fe_3O_4.Al(OH)_3$) NPs were prepared and studied to remove excess fluoride from the aqueous solution. The Langmuir equation evaluated the adsorption capacity and found it to be 88.48 mgg^{-1} at pH 6.5 [22].

Biochar is considered a potential carbon-rich adsorbent due to its high specific surface area and high ion exchange capacity[23]. Lignocellulosic biomass is thermally treated and activated by steaming and subsequently used for several studies to deal with water and wastewaters pollutants removal[24][25]. Pyrolysis technology for converting lignocellulosic biomass into biochar and its modification by treating different chemicals, waste valorization [26] has emerged as a frontier research domain for removing pollutants[27, 28]. Raw biochar, as well as modified biochar, as cost-effective defluoridation agents, are being investigated lately. Thermally treated at 800°C, *Mytilus coruscus* shells (MCS) with fluoride adsorption capacity from 0 to 12.28 mgg^{-1} [29], magnetized corn stover biochar with adsorption capacity 6.42 mg/g [30], Douglas fir biochar (BC) with adsorption capacity 9.0 mgg^{-1} [31] aluminum-modified corn stalk biochar ($AlCl_3$-BC) with adsorption capacity 81.65 mgg^{-1} [32], Zirconium-impregnated *Camellia oleifera* seed shell biochar [33] thermal (torrefaction/pyrolysis) and chemical (iron/zinc) activation of rice husk-derived biochar with adsorption capacity 4.45 mgg^{-1} [34], aluminum-impregnated biochar derived from food waste (Al-FWB) with adsorption capacity 123.4 mgg^{-1} [35], MgAl-mBC biochar with adsorption capacity 21.59 mgg^{-1} [36], Watermelon rind (*Citrullus lanatus*) biochar with adsorption capacity 9.5 mgg^{-1} [37]. The present study investigates the role of biochar derived from Pinus wood for defluoridation.

2. Materials and Methods

2.1. Chemical reagents and adsorbent preparation.

Sodium fluoride was purchased from Sigma Aldrich(St. Louis, Missouri, United States). All chemicals used were of analytical grade unless mentioned otherwise. The *Pinus roxburghii* wood was used as feedstock for biochar (PBC) production. The dried stem was collected from the botanical garden of the university campus, followed by their cutting into fine pieces. Calcium modified biochar (CPBC) was prepared by incubating 50 gm of dried biomass for 24hr in 200 ml, 100mM $CaCl_2$solution. The wet biomass was removed from the calcium solution and sun-dried. The dried biomass was subjected to pyrolysis at high temperature (>400℃) in a muffle furnace and grounded into a fine powder using mortar and

pestle. Control biochar was also prepared in order to investigate the comparative removal of fluoride after calcium modification.

2.2. FT-IR, SEM-EDAX, and fluoride analysis.

ATR-FTIR spectra of the biomass and its modified form were recorded by FTIRspectrometer (Nicolet 6700, Thermo Scientific, MA, USA) at a resolution of 4 $cm^{-1}$to determine the presence and involvement of functional groups that might be present on the surface. The dried powder of biochar was subjected to elemental analysis using a scanning electron microscope (Philips, Netherlands) equipped with Energy Dispersive X-ray System EDAX XL-30, operating at 15-25 KV. Stock solutions of fluoride were prepared by dissolving sodium fluoride in Mili-Q water. Ion chromatography (Metrohm Eco IC, Switzerland) was used to determine the concentration of fluoride. An-ion exchange column and a guard column with a conductivity detector and MSM (Metrohm Suppressor Module) suppressor were used in chromatography. Carbonate (340 mgL^{-1}) and bicarbonate (140mgL^{-1}) were used as the mobile phase, while a rinsing solution of sulphuric acid (5mlL^{-1}) was meant to wash the column after each successive run. In order to load the sample into the column, the injection loop was filled with 10µL of analyte at a flow rate of 0.5 $mLmin^{-1}$. A calibration curve was obtained using sodium fluoride, standard solutions with different concentrations ranging from 2.5 to 10 mgL^{-1}.

2.3. Adsorption experiments.

A batch adsorption experiment was performed in a 200 ml conical Erlenmeyer flask for a comparative study on Pinus biochar (PBC) and calcium modified biochar (CPBC) to remove fluoride. Different parameters influencing adsorption, such as pH, biomass doses, and contact time to optimize fluoride removal, have been carried out. Biomass and analyte were placed at a rotatory orbital shaker operating at 220 rpm at various temperatures. Fluoride solution pH was adjusted by the addition of respective buffer to final concentration 20 mM. Sodium borate buffer was used to maintain pH 2.0 & 3.0, glycine-HCl, pH 4.0 and 5.0, acetate buffer, pH 6.0, citrate buffer, pH 7.0, and phosphate buffer saline for pH 8.0. In order to determine the capacity of adsorption onto PBC and CPBC, 2g of the biochar was placed in 50 mL of fluoride solutions of known concentrations (20mgL^{-1} to 100mgL^{-1}). While, in kinetic studies, fluoride removal by biochar was carried out as a function of contact time with a different initial concentration of sorbate (20, 40, 60, 80, and 100mgL^{-1}) and keeping the adsorbent concentration of 2gL^{-1}. At the end of each adsorption aliquot of the filtrate was obtained using filter paper, Whatman No.1 with pore size 11 µm. Samples were analyzed at certain time intervals between 5 to 60 minutes. Further, the effect of the temperature was investigated by conducting the experiments at six different temperatures (28, 32, 36, 40, 42, and 48°C) in order to obtain thermodynamic parameters.

The percentage sorption of fluoride was calculated by the following equation:

$$\%\, Sorption = \frac{C_{i-}C_e}{C_i} \times 100 \qquad (1)$$

The sorption capacity is the calculated amount of fluoride adsorbed per gram of biochar (mgg^{-1}) as follows:

$$q_e\left(\frac{mg}{g}\right) = \frac{C_i-C_e}{M} \times V \qquad (2)$$

where C_i and C_f are the initial and final concentrations of fluoride in the aqueous solution (mgL^{-1}). V is the volume (L) of the test solution, and M(g) is the mass of biochar, PBC, and CPBC.

3. Results and Discussion

3.1. FT-IR, SEM and EDAX studies.

FT-IR analysis was carried out to identify the interaction among a functional group of biochar and fluoride ions. Figure 1a shows the spectrum of the biochar before adsorption, Figure 1b shows the spectrum of calcium-treated biochar, and Figure 1c shows the spectrum of fluoride-loaded biochar. The peak at 3350 cm^{-1} in untreated biochar was shifted at 3300 in calcium treated biochar, and it further shifts to 3275 cm^{-1} after F^- ion sorption with reduced peak intensity indicating the involvement of –OH stretch of the polymeric group. Peak positioned at 1560 cm^{-1} in biochar is shifted with reduced height 1550 in case of calcium treated biochar. It shifts again to 1545 cm^{-1} in case of fluoride-loaded biomass suggested the involvement of secondary amine >NH functional occurring on to the surface of calcium treated biochar. A similar finding, e.g., involvement of –OH and the amino group, has been reported in the case of fluoride adsorption by biochar derived from waste peanut hull [38]. Similarly, the peak at 1325 was is found to be almost diminished in the case of calcium treatment and shifted to 1345 cm^{-1} after sorption of fluoride ions. This change in intensity and shift of peaks can be attributed to aromatic nitro $–NO_2$ group involvement. The peak at 692 cm^{-1} in calcium treated biochar was shifted 705 cm^{-1}, which can be attributed to the involvement of alkyne (C-H) bend of the biochar after F^- ions adsorption.

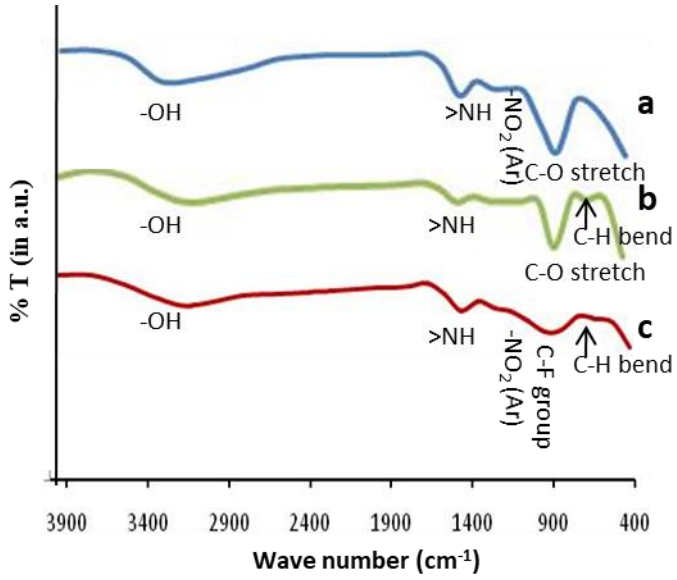

Figure 1. FT-IR spectra of biochar from *P. roxburghii*: (**a**), the spectrum of untreated biochar; (**b**) after calcium pretreatment and (**c**) and after sorption of fluoride ions.

SEM analysis of calcium treated biochar, as well as fluoride, sorbed biochar, is shown in Figures 2a and 2b. The result indicated a porous structure of biochar char. The image clearly reveals the porosity and surface texture, providing adsorbents with large surface areas and high adsorption capacity. The elemental compositions of calcium treated biochar CPBC, and fluoride sorbed CPBC was determined using EDAX analysis (Fig. 2c and d). The result clearly shows the adsorption of fluoride ions onto CPBC with a proportion of F (6%) in nanoparticles followed by carbon (72%), oxygen (20%), and calcium (2%).

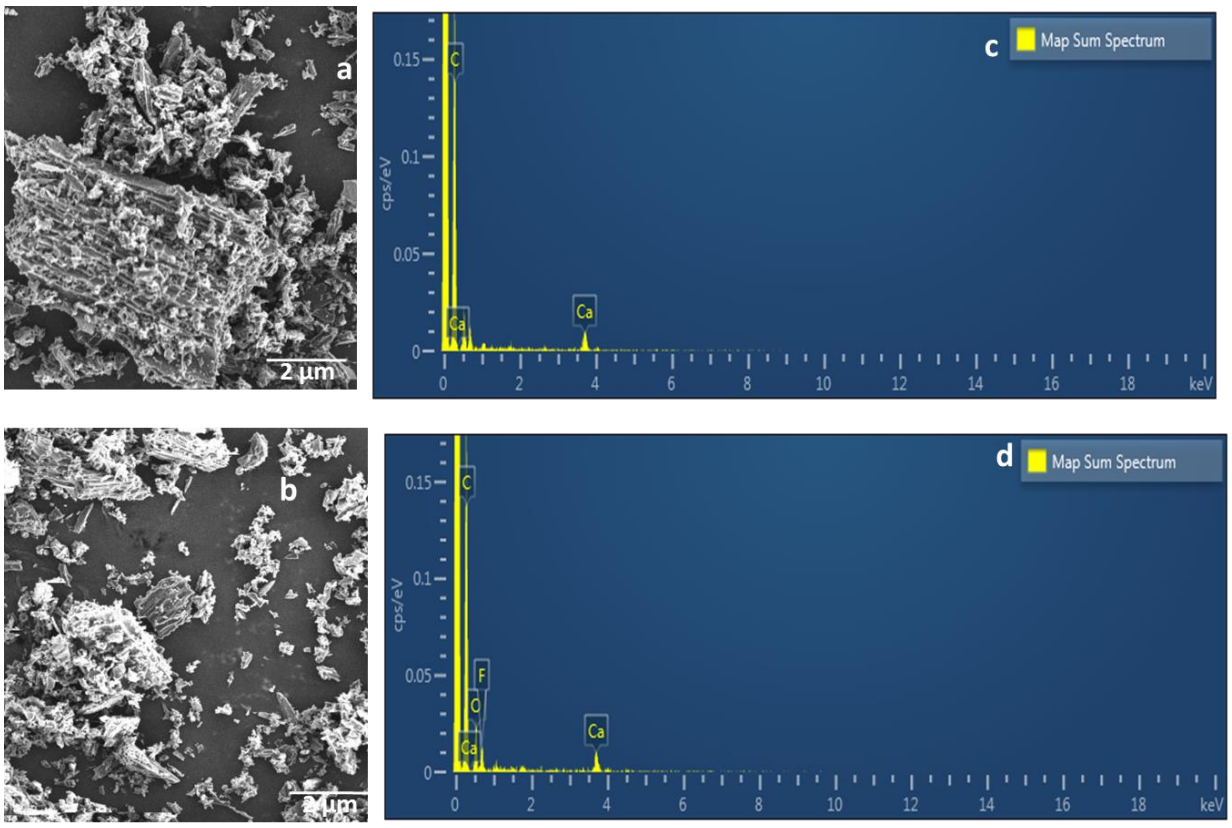

Figure2. (**a**)SEM image of CPBC, showing a highly porous structure of the biochar. Image of biochar after the adsorption of fluoride ions; (**b**) EDAX spectrum showing incorporation of Ca in biochar; (**c**) EDAX spectrum obtained after fluoride sorption onto CPBC.

3.2. Effect of pH, contact time, and adsorbent doses on adsorption.

Fluoride ion sorption was studied for the determination of maximum removal at different pH. The maximum percentage removal was found to be at pH 4.5 (Figure 3a). At low pH surface of calcium modified biochar are positively charged and attracted towards negatively charged fluoride ions.

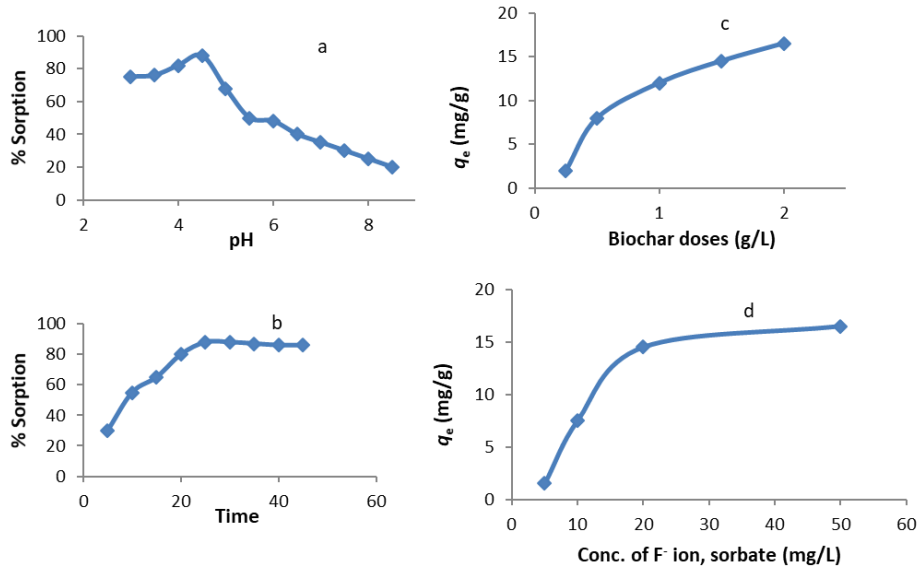

Figure3.(**a**) Effect of pH, where optimum pH was found to be 4.5; (**b**) Effect of contact time on sorption of fluoride onto sorbent (F^{-1} 50 mg/L, sorbate concentration: 2g/L at 30°C);(**c**) The effect of biochar doses and (**d**) effect of fluoride concentration on overall sorption processes at 30°C.

Low pH has been found to be favorable for fluoride adsorption [29]. Contact time's effect on fluoride ions' sorption onto CPBC was studied using sorbent doses 2.0 gL^{-1} and sorbate 50 mg L^{-1} at room temperature (Figure 3b). The maximum sorption of fluoride (86.52%) was observed after mixing sorbate and sorbent for a period of 25 min. Figure 3c, shows the pattern for absorption of fluoride for a different dose of sorbent. Maximum sorption occurred when 2 gL^{-1} of CPBC was subjected to sorption studies. An increase in fluoride concentration to more than 50 m L^{-1}, when sorbent doses were2g/L, did not enhance overall sorption in the batch sorption model (Figure 3d).In a study, Al-impregnated food waste biochar removed fluoride 91.4% [35]. Rice husk biochar has been reported to defluoridation solution to the extent of 95.4% [34].

3.3. Adsorption isotherms.

Three equilibrium models, namely Langmuir, Freundlich, and Dubinin-Radushkevich (D-R) isotherm models, have been applied to investigate the sorption studies. The Langmuir model hypothesizes a monolayer adsorption process without any interaction between sorbed ions. A none linear Langmuir isotherm is described by the following formula:

$$q_e = \frac{q_m K_L C_e}{1+K_L C_e} \quad (3)$$

where q_e is the equilibrium fluoride ion concentration on the CPBC (mg/g), C_e is the equilibrium metal ion concentration in the solution (mgL^{-1}), q_m is the monolayer biosorption capacity of the adsorbent (mgg^{-1}), and K_L is the Langmuir biosorption constant (Lmg^{-1}), relating the free energy of sorption. A nonlinear relationship of F^- ions were sorbed per unit sorbent. The coefficient of determination (R^2) was found to be 0.914 for F^- ion sorption (Figure 4a). The maximum sorption capacity (q_m) of the sorbent was found to be 16.72 mgg^{-1}, while K_L value was calculated as 0.0125 Lmg^{-1} for F^-ions. The Freundlich model assumes a heterogeneous adsorption surface and active sites with different energy. This isotherm can be explained by the following formula:

$$q_e = K_f C_e^{1/n} \quad (4)$$

where K_f is a constant relating to the fluoride sorption capacity, and $1/n$ is an empirical parameter relating to fluoride sorption intensity depending upon the heterogeneity of the material. A Freundlich isotherm was obtained by plotting q_eVs. C_e values, which showing a nonlinear relationship. The 0.885 R^2 value indicated that the Freundlich model could not describe the relationship between the amounts of sorbed fluoride ions adequately to their equilibrium concentration in the solution. The Langmuir isotherm model best fitted the equilibrium with a higher R^2 value than the Freundlich model. The physical or chemical nature of fluoride sorption processes was examined by analyzing the D-R isotherm model's equilibrium data. The linear form of D-R isotherm model is presented by the following equation:

$$\ln q_e A = \ln q_m - \beta\varepsilon^2 \quad (5)$$

where β is the activity coefficient related to mean sorption energy (mol^2/J^2) and ε is the Polanyi potential $\varepsilon = RT \ln (1 + 1/C_e)$. The D-R isotherm model well fitted the equilibrium data since the R^2 value was found to be 0.997 for F^- ions sorption (Figure 4b). Sorption means free energy (E; kJ/mol) gives adsorption's physical or chemical nature. The mean sorption energy (E; kJ/mol) is expressed as follows:

$$E = \frac{1}{\sqrt{2\beta}} \quad (6)$$

When values lie between 8 and 16 kJ/mol, the adsorption process is regarded as chemical. Similarly, adsorption is physical when Evalue is less than 8 kJ/mol. The mean sorption energy was calculated as 9.27 for fluoride ions suggesting a chemisorptions type of sorption.

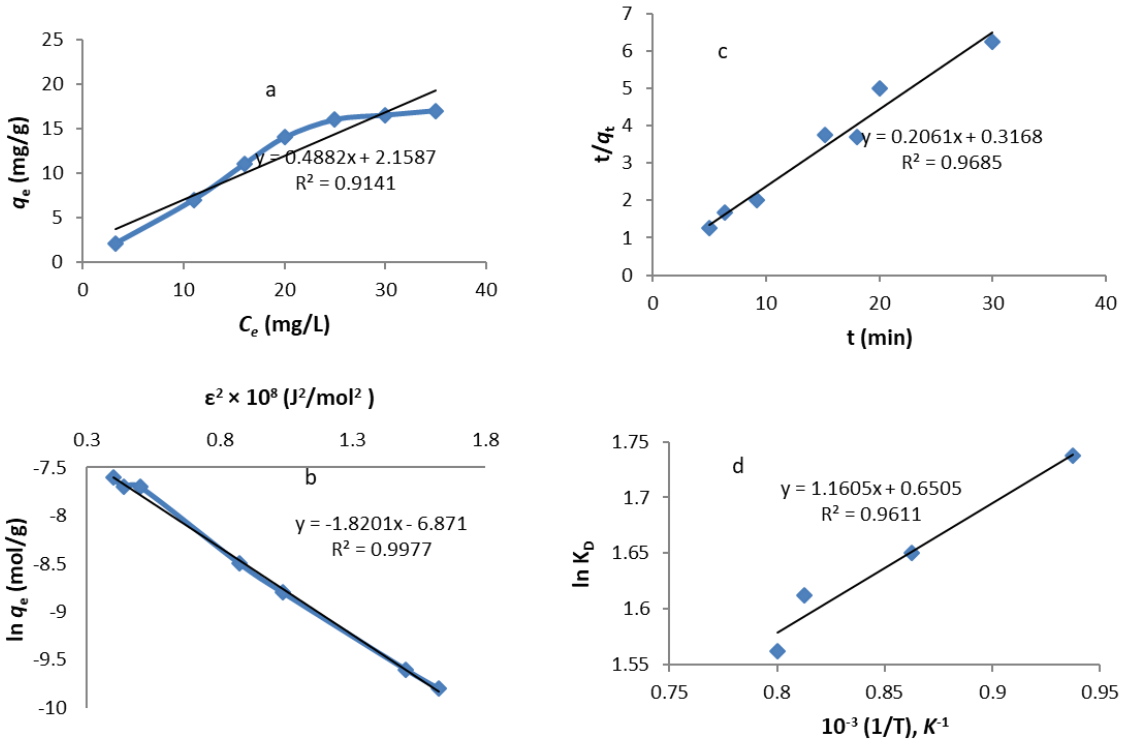

Figure 4. (**a**)Langmuir isotherm plots for sorption of fluoride onto CPBC;(**b**) D-R isotherm plots for sorption of fluoride;(**c**) Second-order sorption kinetic models for fluoride ions uptake;(**d**) Plot of ln K_D Vs. 1/T for the estimation of thermodynamic parameters.

3.4. Adsorption kinetic models.

Pseudo-first order and Pseudo-second order kinetic models were used to analyze the sorption rate of fluoride ions onto CPBC biochar. The pseudo-first-order rate equation is given as follows:

$$\log (q_e - q_t) = \frac{\log q_e - k_t t}{2.303} \qquad (7)$$

where q_e (mgg^{-1}) is the amount of metal ions sorbed at equilibrium and q_t is the amount of metal sorbed at any time (mgg^{-1}), and k_1 is the rate constant of the equation (min^{-1}). The biosorption rate constant $k_1$can be can be determined experimentally by plotting log (q_e-q_t) versus t. Experimental data were also tested by pseudo-second-order equation.

$$\frac{t}{q_t} = \frac{1}{k_2 q_e^2} + (\frac{1}{q_e})t \qquad (8)$$

where k_2 is the equilibrium rate constant ($gmg^{-1}min^{-1}$). The values of the correlation coefficient of the pseudo-second-order model were found to be 0.968 for F^{-1} ions, which is higher than the pseudo-first-order model i.e., 0.832 (Figure 4c). The pseudo-second-order model can explain the kinetic behavior of F^{-1}ions onto CPBC satisfactorily with a good correlation coefficient.

3.5. Biosorption thermodynamics.

The thermodynamic parameters including the change in free energy (ΔG°), enthalpy (ΔH°) and entropy (ΔS°) by analyzing D-R isotherm plotting. The change in free energy (ΔG°) was calculated from the following equations:

$$G^{\circ} = -\mathrm{RT}\ln \mathrm{K_D} \qquad (9)$$

where, Ris the universal gas constant (8.314 J/mol K), T is the temperature (K), and K_D (q_e/C_e) is the distribution coefficient. The enthalpy (ΔH°) and entropy (ΔS°) parameters were estimated from the following equation:

$$\ln \mathrm{K_D} = \left(\frac{\Delta S^{o}}{T}\right) - \left(\frac{\Delta H^{o}}{RT}\right) \qquad (10)$$

The slope and intercept of the plot of ln K_D versus 1/*T* give a value of ΔH° and ΔS°. Gibbs free energy change (ΔG°) was found to be -15.34, -15.05, -14.98, and −14.23 kJ/mol for fluoride adsorption at 20, 30, 40, and 50°C, respectively (fig.4d). The thermodynamically feasible and spontaneous nature of the sorption is denoted by negative ΔG°values. Lesser feasibility of sorption at high temperatures is found as there is a decrease in ΔG° values with increased temperature. The enthalpy of biosorption ΔH° parameter was found to be −21.44 in the case of fluoride sorption on CPBC. The negative ΔH° indicates the exothermic nature of sorption at 20 to 50°C. The enthalpy or the heat of sorption ranging from 2.1 to 20.9 KJ/mol corresponds to physical sorption, whereas ranging from 20.9 to 418 KJ/mol is regarded as chemical sorption. Therefore the ΔH° value suggested that the sorption process of F^{-1} occurred due to chemisorptions. The ΔS°parameter was found to be −15.34J/molK for fluoride sorption, suggested a decrease in the randomness at the solid/solution interface during the sorption process.

4. Conclusions

Calcium pretreated *Pinus roxburghii* biochar was employed as an adsorbent for the removal of F^{-1} ions from an aqueous solution. In batch sorption studies maximum sorption capacity of prepared sorbent was found to be 16.72 $mgg^{-1}$for fluoride ions at optimal experimental conditions. The FT-IR analysis indicated the involvement of functional groups (-OH, $>NH_2$, $-NO_2$, C-F, and C-H) in fluoride sorption processes. Langmuir model was well fitted, suggesting monolayer adsorption while experimental adsorption data followed pseudo-second-order kinetics. The free energy from the D-R isotherm model indicated that the sorption of fluoride ions onto CPBC primarily occurred due to chemisorptions. This low-cost biochar can be used for the removal of fluoride from potable water.

Funding

The work did not receive any grant.

Acknowledgments

KSP would like to acknowledge the help rendered by technical assistants of the Center of Environmental Science, IIDS, UoA, Prayagraj, India.

Conflicts of Interest

The authors declare no conflict of interest.

References

1. Vörösmarty, C.J.; McIntyre, P.B.; Gessner, M.O.; Dudgeon, D.; Prusevich, A.; Green, P.; *et al*. Global threats to human water security and river biodiversity. *Nature* **2010**, *467*, 555–61, https://doi.org/10.1038/nature09440.
2. Mandal, B.; Chowdhury, T.; Samanta, G.; Mukherjee, D.; Chanda, C.; Saha, K.; *et al*. Impact of safe water for drinking and cooking on five arsenic-affected families for 2 years in West Bengal, India. *Sci Total Environ* **1998**, *218*, 185–201, https://doi.org/10.1016/S0048-9697(98)00220-4.
3. Brindha, K.; Rajesh, R.; Murugan, R.; Elango, L. Fluoride contamination in groundwater in parts of Nalgonda District, Andhra Pradesh, India. *Environ Monit Assess* **2011**, *172*, 481–92.
4. Ibrahim, M.; Asimrasheed, M.; Prabhakar, P. Effects of fluoride contents in groundwater : A review. *Int J Pharm Appl* **2011**, *2*, 128–34.
5. Kumar, P.; Kumar, C.; Saraswat, C.; Mishra, B. Evaluation of aqueous geochemistry of fluoride enriched groundwater : A case study of the Patan district , Gujarat , *Western. Water Sci* **2017**, *31*, 215–29, https://doi.org/10.1016/j.wsj.2017.05.002.
6. Bhupinder, S. Assessment of groundwater quality with respect to fluoride. *Univers J Environ Res* **2011**, *1*, 45–50.
7. Amini, M.; Mueller, K.; Abbaspour, K.C.; Rosenberg, T.; Afyuni, M.; Møller, K.N.; *et al*. Statistical modeling of global geogenic fluoride contamination in groundwaters. *Environ Sci Technol* **2008**, *42*, 3662–8, https://doi.org/10.1021/es071958y.
8. Shah, T. Groundwater and human development: challenges and opportunities in livelihoods and environment. *Water Sci Technol* **2005**, *51*, 27–37, https://doi.org/10.2166/wst.2005.0217.
9. Gaciri, S.J.; Davies, T.C. The occurrence and geochemistry of fluoride in some natural waters of Kenya. *J Hydrol* **1993**, *143*, 395–412, https://doi.org/10.1016/0022-1694(93)90201-J.
10. Awadia, A.K.; Birkeland, J.M.; Haugejorden, O.; Bjorvatn, K. An attempt to explain why Tanzanian children drinking water containing 0.2 or 3.6 mg fluoride per liter exhibit a similar level of dental fluorosis. *Clin Oral Investig* **2000**, *4*, 238–44.
11. Daifullah, A.A.M.; Yakout, S.M.; Elreefy, S.A. Adsorption of fluoride in aqueous solutions using KMnO4-modified activated carbon derived from steam pyrolysis of rice straw. *J Hazard Mater* **2007**, *147*, 633–43, https://doi.org/10.1016/j.jhazmat.2007.01.062.
12. Wu, H.; Chen, L.; Gao, G.; Zhang, Y.; Wang, T.; Guo, S. Treatment effect on the adsorption capacity of alumina for removal fluoride. *Nano Biomed Eng* **2010**, *2*, 231–5, https://doi.org/10.5101/nbe.v2i4.p231-235.
13. Meenakshi; Garg, V.K.; Kavita; Renuka; Malik, A. Groundwater quality in some villages of Haryana, India: focus on fluoride and fluorosis. *J Hazard Mater* **2004**, *106*, 85–97.
14. Prasad, K.S.; Amin, Y.; Selvaraj, K. Defluoridation using biomimetically synthesized nano zirconium chitosan composite: Kinetic and equilibrium studies. *J Hazard Mater* **2014**, *276*, 232-240, https://doi.org/10.1016/j.jhazmat.2014.05.038.
15. He, J.; Yang, Y.; Wu, Z.; Xie, C.; Zhang, K.; Kong, L. *et al*. Review of fluoride removal from water environment by adsorption. *J Environ Chem Eng* **2020**, *8*, 104516. https://doi.org/10.1016/j.jece.2020.104516.
16. Raichur, A.M.; Jyoti Basu, M. Adsorption of fluoride onto mixed rare earth oxides. *Sep Purif Technol* **2001**, *24*, 121-127, https://doi.org/10.1016/S1383-5866(00)00219-7.
17. Hamamoto, S.; Kishimoto, N. Characteristics of fluoride adsorption onto aluminium(III) and iron(III) hydroxide flocs. *Sep Sci Technol* **2017**, *52*, 42–50, https://doi.org/10.1080/01496395.2016.1242628.
18. Nabbou, N.; Belhachemi, M.; Boumelik, M.; Merzougui, T.; Lahcene, D.; Harek, Y.; *et al*. Removal of fluoride from groundwater using natural clay (kaolinite): Optimization of adsorption conditions. *Comptes Rendus Chim* **2019**, *22*, 105–12, https://doi.org/10.1016/j.crci.2018.09.010.
19. He, Y.; Zhang, L.; An , X.; Wan, G.; Zhu, W.; Luo, Y. Enhanced fluoride removal from water by rare earth (La and Ce) modified alumina: Adsorption isotherms, kinetics, thermodynamics and mechanism. *Sci Total Environ* **2019**, *688*, 184–98, https://doi.org/10.1016/j.scitotenv.2019.06.175.
20. Pillai, P.; Dharaskar, S.; Shah, M.; Sultania, R. Determination of fluoride removal using silica nano adsorbent modified by rice husk from water. *Groundw Sustain Dev* **2020**, *11*, 100423, https://doi.org/10.1016/j.gsd.2020.100423.
21. Vijila, B.; Edinsha Gladis, E.H.; Michael, Ahitha; Jose, J.; Sharmila, T.M.; Joseph, J. Removal of fluoride with rice husk derived adsorbent from agro waste materials. *Mater Today Proc* **2021**, *45*, 2125–2129,

https://doi.org/10.1016/j.matpr.2020.09.729.
22. Zhao, X.; Wang, J.; Wu, F.; Wang, T.; Cai, Y.; Shi, Y. *et al*. Removal of fluoride from aqueous media by Fe3O4@Al(OH)3 magnetic nanoparticles. *J Hazard Mater* **2010**, *173*,102–119, https://doi.org/10.1016/j.jhazmat.2009.08.054.
23. Liu, J.; Jiang, J.; Meng, Y.; Aihemaiti, A.; Xu, Y.; Xiang, H. *et al*. Preparation, environmental application and prospect of biochar-supported metal nanoparticles: A review. *J Hazard Mater* **2020**, *388*, 122026, https://doi.org/10.1016/j.jhazmat.2020.122026.
24. Othmani, A.; John, J.; Rajendran, H.; Mansouri, A.; Sillanpää, M.; Velayudhaperumal Chellam, P. Biochar and activated carbon derivatives of lignocellulosic fibers towards adsorptive removal of pollutants from aqueous systems: Critical study and future insight. *Sep Purif Technol* **2021**, *274*, 119062, https://doi.org/10.1016/j.seppur.2021.119062.
25. Kamali, M.; Appels, L.; Kwon, E.E.; Aminabhavi, T.M.; Dewil, R. Biochar in water and wastewater treatment - a sustainability assessment. *Chem. Eng. J.* **2021**, *420*, 129946, https://doi.org/10.1016/j.cej.2021.129946.
26. Kang, J.K.; Seo, E. J.; Lee, C.G.; Park, S.J. Fe-loaded biochar obtained from food waste for enhanced phosphate adsorption and its adsorption mechanism study via spectroscopic and experimental approach. *J Environ Chem Eng* **2021**, *9*, 105751, https://doi.org/10.1016/j.jece.2021.105751.
27. Yaashikaa, P.R.; Senthil Kumar, P.; Varjani, S.J.; Saravanan, A. Advances in production and application of biochar from lignocellulosic feedstocks for remediation of environmental pollutants. *Bioresour Technol* **2019**, *292*, 122030, https://doi.org/10.1016/j.biortech.2019.122030.
28. Yi, Y.; Huang, Z.; Lu, B.; Xian, J.; Tsang, E.P.; Cheng, W. *et al*. Magnetic biochar for environmental remediation: A review. *Bioresour Technol* **2019**, *298*, 122468, https://doi.org/10.1016/j.biortech.2019.122468.
29. Lee, J.I.; Kang, J.K.; Hong, S.H.; Lee, C.G.; Jeong, S.; Park, S.J. Thermally treated Mytilus coruscus shells for fluoride removal and their adsorption mechanism. *Chemosphere* **2021**, *263*, 128328, https://doi.org/10.1016/j.chemosphere.2020.128328.
30. Mohan, D.; Kumar, S.; Srivastava, A. Fluoride removal from ground water using magnetic and nonmagnetic corn stover biochars. *Ecol Eng* **2014**, *73*, 798–808, https://doi.org/10.1016/j.ecoleng.2014.08.017.
31. Bombuwala Dewage, N.; Liyanage, A.S.; Pittman, C.U.; Mohan, D.; Mlsna, T. Fast nitrate and fluoride adsorption and magnetic separation from water on A-Fe2O3 and Fe3O4 dispersed on Douglas fir biochar. *Bioresour Technol* **2018**, *263*, 258–65, https://doi.org/10.1016/j.biortech.2018.05.001.
32. Zhang, X.; Qi, Y.; Chen, Z.; Song, N.; Li, X.; Ren, D. *et al*. Evaluation of fluoride and cadmium adsorption modification of corn stalk by aluminum trichloride. *Appl Surf Sci* **2021**, *543*, 148727, https://doi.org/10.1016/j.apsusc.2020.148727.
33. Mei, L.; Qiao, H.;, Ke, F.; Peng, C.; Hou, R.; Wan, X., *et al*. One-step synthesis of zirconium dioxide-biochar derived from *Camellia oleifera* seed shell with enhanced removal capacity for fluoride from water. *Appl Surf Sci* **2020**, *509*, 144685, https://doi.org/10.1016/j.apsusc.2019.144685.
34. Yadav, K.; Jagadevan, S. Influence of torrefaction and pyrolysis on engineered biochar and its applicability in defluoridation: Insight into adsorption mechanism, batch adsorber design and artificial neural network modelling. *J Anal Appl Pyrolysis* **2021**, *154*, 105015, https://doi.org/10.1016/j.jaap.2021.105015.
35. Meilani, V.; Lee, J.I.; Kang, J.K.; Lee, C.G.; Jeong, S.; Park, S.J. Application of aluminum-modified food waste biochar as adsorbent of fluoride in aqueous solutions and optimization of production using response surface methodology. *Microporous Mesoporous Mater* **2021**, *312*, 110764, https://doi.org/10.1016/j.micromeso.2020.110764.
36. Shen, Z.; Jin, J.; Fu, J.; Yang, M.; Li. F. Anchoring Al- and/or Mg-oxides to magnetic biochars for Co-uptake of arsenate and fluoride from water. *J Environ Manage* **2021**, *293*, 112898, https://doi.org/10.1016/j.jenvman.2021.112898.
37. Sadhu, M.; Bhattacharya, P.; Vithanage, M.; Padmaja Sudhakar, P. Adsorptive removal of fluoride using biochar – a potential application in drinking water treatment. *Sep Purif Technol* **2021**, 119106, https://doi.org/10.1016/j.seppur.2021.119106.
38. Kumar, P.; Prajapati, A.K.; Dixit, S.; Yadav, V.L. Adsorption of fluoride from aqueous solution using biochar prepared from waste peanut hull. *Mater Res Express* **2019**, *6*, 125553, https://doi.org/10.1088/2053-1591/ab6ca0.